

Random large eddy simulation for 3-dimensional incompressible viscous flows

Zihao Guo* and Zhongmin Qian[†]

Abstract

We develop a numerical method for simulation of incompressible viscous flows by integrating the technology of random vortex method with the core idea of Large Eddy Simulation (LES). Specifically, we utilize the filtering method in LES, interpreted as spatial averaging, along with the integral representation theorem for parabolic equations, to achieve a closure scheme which may be used for calculating solutions of Navier-Stokes equations. This approach circumvents the challenge associated with handling the non-locally integrable 3-dimensional integral kernel in the random vortex method and facilitates the computation of numerical solutions for flow systems via Monte-Carlo method. Numerical simulations are carried out for both laminar and turbulent flows, demonstrating the validity and effectiveness of the method.

Key words: large eddy simulation, Monte-Carlo simulation, viscous flows, turbulent flows

MSC classifications: 76M35, 76M23, 60H30, 65C05, 68Q10.

1 Introduction

The idea of utilising statistical mechanics and probabilistic approach is not new in Computational Fluid Dynamics (CFD), although, to the best knowledge of the present authors, it seems that methods such as Monte-Carlo simulation, particle system method of turbulence and other stochastic methods have not been used extensively in industry. While these methods are quite stimulating and there is a high potential of being useful tools in the study of fluid flows including turbulent flow simulation. Among them, the random vortex method (cf. [1], [2] and [8] for details) developed over the last three decades stands out as an important tool, whose successful applications in simulations of incompressible flows however are limited to special flows, mainly are restricted to two dimensional flows. The random vortex method for three dimensional (3D) flows has been developed recently in [11] by using a Feynman-Kac type formula, revealing the difficulty caused by the non-linear stretching term which does not appear in two dimensional flows. Technically, the main problem in the random vortex method for three dimensional incompressible flows lies in the fact the singular integral kernel appearing in the stochastic integral representation is no longer locally integrable, which certainly induces instability of corresponding numerical schemes. Let us recall the key idea in random vortex methods. Let $u(x, t)$ and $p(x, t)$ denote the velocity and the pressure respectively. Then the motion equation of the flow is the Navier-Stokes equations (cf. [5]):

$$\partial_t u + (u \cdot \nabla)u = \nu \Delta u - \nabla p + F$$

and

*Zhongtai Securities Institute for Financial Studies, Shandong University, Jinan, China, 250100, Email: gzhsdu@mail.sdu.edu.cn

[†]Mathematical Institute, University of Oxford, Oxford, United Kingdom, OX2 6GG, and Oxford Suzhou Centre for Advanced Research, Suzhou, China. Email: qianz@maths.ox.ac.uk

$$\nabla \cdot u = 0,$$

where $\nu > 0$ is the kinematic viscosity, and F is an external force applying to the flow. The key observation is that the velocity u can be recovered from the vorticity $\omega = \nabla \wedge u$ through the Biot-Savart law by integrating the vorticity against a singular integral kernel $K(y, x)$. In fact, K is the gradient of the Green function, and therefore K is a nice kernel for integration. While for three dimensional flows, a further derivative of the Biot-Savart kernel K is required, which is not locally integrable unfortunately. This difficulty originates from the random vortex method which aims to calculate numerically the vorticity ω first based on the vorticity transport equation

$$\partial_t \omega + (u \cdot \nabla) \omega = \nu \Delta \omega + (\omega \cdot \nabla) u + \nabla \wedge F$$

and the velocity u is recovered from ω . Let us recall the technical steps briefly for two dimensional flows and the external vorticity $\nabla \wedge F = 0$ to motivate our approach in the present paper. For this case, the non-linear stretching term $(\omega \cdot \nabla) u$ vanishes identically. Let X be Brownian fluid particles X with velocity $u(x, t)$. That is, according to Taylor's Brownian motion X is determined by stochastic differential equation

$$dX_t = u(X_t, t)dt + \sqrt{2\nu}dB_t, \quad X_0 = \xi. \quad (1.1)$$

To avoiding confusion, the notation X^ξ denotes Brownian fluid particles issued from a location ξ . Since ω is a solution of the vorticity transport equation, an easy exercise shows that

$$\omega(y, t) = \int h(0, \xi; t, y) u_0(\xi) d\xi,$$

where $h(s, x; t, y)$ (for $s < t$) is the transition probability function of the Taylor diffusion X , cf. [15]. Together with the Biot-Savart law and the Fubini theorem we may represent the velocity

$$u(x, t) = \int K(y, x) \omega(y, t) dy = \int \left[\int K(y, x) h(0, \xi; t, y) dy \right] u_0(\xi) d\xi.$$

Now the integral with respect to y , that is, $\int K(y, x) h(0, \xi; t, y) dy$ is the average $\mathbb{E} [K(X_t^\xi, x)]$, so that $u(x, t) = \int \mathbb{E} [K(X_t^\eta, x)] u_0(\eta) d\eta$, which allows to reformulate the equation for X as a stochastic differential equation of Vlasov-McKean type

$$dX_t^\xi = \left(\int \mathbb{E} [K(X_t^\eta, x)] u_0(\eta) d\eta \Big|_{x=X_t^\xi} \right) dt + \sqrt{2\nu} dB_t, \quad X_0^\xi = \xi$$

on which numerical schemes may be developed accordingly for calculating two dimensional flows. The idea similarly applies to three dimensional flows but unfortunately involves the gradient of K which is not locally integrable. See more details about random vortex method and integral representation theorem in [6], [11] and [12].

There are mainly two difficulties in numerically solving fluid dynamic equations of turbulent flows, which are non-linear characteristics of the Navier-Stokes equation and continuously changing complex vortices of different scales. In engineering applications, people are more concerned about the time-averaged effect of turbulent motion, so some of the commonly used turbulence models are based on Reynolds time averaging, called Reynolds Average Numerical Simulation (RANS). RANS smooths out some tiny details of turbulent motion, and the model has many artificial settings. Therefore, RANS models have limited simulation capabilities for complex and delicate turbulent structure such as the separation phenomena of flow past body. With the increasing of the computing power and computer memory capacity, some advanced research institutions solve the Navier-Stokes equations without any form of simplification, but use extremely fine grids to directly numerically solve the Navier-Stokes

equations. This kind of approach may be called Direct Numerical Simulation (DNS). However, DNS are still computational expensive to implement. The Large Eddy Simulation (LES) method, which is between DNS and the RANS method, has gradually emerged in the computational fluid dynamics community and has developed into a promising method for numerically solving turbulent flows because it is more sophisticated than the RANS and can be implemented on a conventional computer.

LES is considered as a useful tool for numerically simulating turbulent flows (cf. [7] and [16]). The principal idea in LES is to reduce the computational cost by ignoring the eddies in small length scales, which are very expensive in numerical experiments, via filtering of the Navier–Stokes equations. Such filtering, which can be viewed as spatial-averaging, effectively removes the information of eddies in small-scale from the numerical solution, for original ideas, cf. [3] and [13]. The filtered velocity $\tilde{u}(x, t)$ can be represented as

$$\tilde{u}(x, t) = \int_{\mathbb{R}^3} \chi(x - x') u(x', t) dx'$$

where $x, x' \in \mathbb{R}^3$, $\chi(x, t)$ is the filtering function including top-hat function, Gaussian function and so on, which satisfies $\int \chi(x) dx = 1$. So the filtered Navier-Stokes equation becomes

$$\partial_t \tilde{u} + \widetilde{(u \cdot \nabla) u} = \nu \Delta \tilde{u} - \nabla \tilde{p} + \tilde{F}$$

and

$$\nabla \cdot \tilde{u} = 0,$$

Because $\widetilde{(u \cdot \nabla) u}$ can not be simplified as $(\tilde{u} \cdot \nabla) \tilde{u}$, so researcher introduced sub-grid-scale stress τ , defined as

$$\nabla \cdot \tau = (\tilde{u} \cdot \nabla) \tilde{u} - \widetilde{(u \cdot \nabla) u}$$

The filtered Navier-Stokes equation can be rewritten as

$$\partial_t \tilde{u} + (\tilde{u} \cdot \nabla) \tilde{u} = \nu \Delta \tilde{u} - \nabla \tilde{p} + \tilde{F} - \nabla \cdot \tau$$

The τ means the effect of small eddies on the flow system which must be modelled because its information is not irrelevant. The influence of small-scale eddies on the equation of motion is described by some other models (cf. [9], [14] and [10]), but it is not the studying target of our paper. Through large eddy simulation, the filtered equations focus on analysing large-scale eddies, directly capturing the most important turbulent structure and dynamical information, while approximating small-scale eddies. This method effectively reduces the computational complexity and retains the main physical properties.

Random large eddy simulation method we developed in this paper combines the core idea of filtering in large eddy simulation with the integral representation of parabolic equation in random vortex method, and subsequently obtain the numerical method of incompressible viscous flows based on it. Using the stochastic integral representation of parabolic equation and basic idea of large eddy simulation, we are able to close the solution of Navier-Stokes equation, which makes it possible for us to simulate incompressible flows via Monte-Carlo method.

The paper is organised as follows. In Section 2, we propose the random large eddy simulation method based on stochastic integral representation and large eddy simulation. Then, numerical schemes and simulation experiments are presented in Section 3. Finally, we introduce conditional law duality and integral representation theorem in Appendix, which is the theoretical foundation of the random large eddy simulation method established in Section 2.

2 Random large eddy simulation method

The present work aims to implement the ideas of random vortex method described in the introduction directly to the velocity rather than through the vorticity equation, so that the method developed in the

present paper works for three dimensional (turbulent) flows as well. Firstly, for an incompressible flow, the divergence of the velocity vanishes: $\nabla \cdot u = 0$, which implies that the probability transition function $p(s, x; t, y)$ is the fundamental solution for the backward parabolic operator $\partial_t + v\Delta + u \cdot \nabla$, so it is also the fundamental solution of the forward parabolic operator $\partial_t - v\Delta + u \cdot \nabla$. Therefore $u(x, t)$ has the following implicit integral representation

$$u(x, t) = \int_{\mathbb{R}^3} p(0, \eta; t, x) u_0(\eta) d\eta + \int_0^t \int_{\mathbb{R}^3} h(s, \eta; t, x) (-\nabla h(\eta, s) + F(\eta, s)) d\eta ds \quad (2.1)$$

where ∇p can be calculated by using the Biot-Savart law. In fact, since $\nabla \cdot u = 0$, the pressure $p(x, t)$ at every instance t satisfies the Poisson equation

$$\Delta p = - \sum_{i,j=1}^3 \frac{\partial u^j}{\partial x^i} \frac{\partial u^i}{\partial x^j} + \nabla \cdot F$$

so that, according to Green formula,

$$p(x, t) = \int_{\mathbb{R}^3} G_3(y, x) \left(- \sum_{i,j=1}^3 \frac{\partial u^j}{\partial x^i} \frac{\partial u^i}{\partial x^j} + \nabla \cdot F \right) \Big|_{(y,t)} dy$$

where $G_3(y, x) = -\frac{1}{4\pi} \frac{1}{|y-x|}$ is the Green function on \mathbb{R}^3 . Differentiating under integration (which we assume is legible) to deduce that

$$\nabla p(x, t) = \int_{\mathbb{R}^3} K_3(y, x) \left(\sum_{i,j=1}^3 \frac{\partial u^j}{\partial x^i} \frac{\partial u^i}{\partial x^j} - \nabla \cdot F \right) \Big|_{(y,t)} dy, \quad (2.2)$$

where

$$K_3(y, x) = -\nabla_x G_3(y, x) = \frac{1}{4\pi} \frac{y-x}{|y-x|^3} \quad \text{for } y \neq x$$

is the Biot-Savart kernel. The representation (2.2) shall be used to update the pressure $p(x, t)$ in solving numerically the velocity $u(x, t)$ via the Navier-Stokes equations.

For simplicity we set $g = -\nabla p + F$. For every ξ and instance $t \geq 0$, X_t^ξ denotes the position in the state space of the Brownian fluid particles with velocity $u(x, t)$ started from ξ , and $X : (t, \xi) \rightarrow X_t^\xi$ defines a random field. In terms of the law of random field X , (2.1) can be written formally as

$$u(x, t) = \int_{\mathbb{R}^3} \mathbb{E} [\delta_x(X_t^\eta)] u_0(\eta) d\eta + \int_0^t \int_{\mathbb{R}^3} \mathbb{E} [\delta_x(X_t^\eta) | X_s^\eta] g(\eta, s) d\eta ds \quad (2.3)$$

by using the formal symbol $h(0, \eta; t, x) = \mathbb{P} [X_t^\eta = x]$. The problem here is that of course $\delta_x(X_t^\eta)$ is a generalised Wiener functional so that it is difficult to calculate it numerically. Also the conditional average $\mathbb{E} [\delta_x(X_t^\eta) | X_s^\eta]$ is expensive to compute. To overcome these difficulties, we utilise a key idea from the approach of Large Eddy Simulations (LES). In LES, one calculates local averaged velocity which shall give the global structure of the flow (in particular for turbulent flows). We shall adopt the LES approach, avoiding the modelling of the error term caused by taking local average of the velocity.

To realise this scheme, we shall use a stochastic integral representation for solutions of a linear parabolic equation. Since u is a solution to

$$(v\Delta - u \cdot \nabla - \partial_t) u + g = 0, \quad (2.4)$$

according to the representation theorem (4.1) to be established in Appendix

$$u(x, t) = \int_{\mathbb{R}^3} h(0, \eta; t, x) u_0(\eta) d\eta + \int_0^t \int_{\mathbb{R}^3} \mathbb{E} [g(X_s^\eta, s) | X_t^\eta = x] h(0, \eta, t, x) d\eta ds. \quad (2.5)$$

Comparing with (2.3), the difference seems not so significant, and indeed the two representations are equivalent due to the assumption that $\nabla \cdot u = 0$, while (2.5) involves only Brownian fluid particles started at the same instance, which in fact greatly reduces the computational cost.

By borrowing the key idea in LES, a filter function χ with a compact support is applied for calculating the local average of the velocity, denoted by $\tilde{u}(x, t)$. More precisely,

$$\tilde{u}(x, t) = \int_{\mathbb{R}^3} \chi(\xi - x) u(\xi, t) d\xi \quad (2.6)$$

where $x \in \mathbb{R}^3$. In the present paper, we choose a parameter $s > 0$ as the mesh size, the filter function used in the paper is Gaussian kernel $\chi(x) = \left(\frac{6}{\pi s^2}\right)^{\frac{3}{2}} e^{-\frac{6|x|^2}{s^2}}$ for $x \in \mathbb{R}^3$.

Combining (2.5) and (2.6), we may easily obtain the following functional integral representation

$$\begin{aligned} \tilde{u}(x, t) &= \int_{\mathbb{R}^3} \mathbb{E} [\chi(X_t^\eta - x)] u_0(\eta) d\eta \\ &+ \int_0^t \int_{\mathbb{R}^3} \mathbb{E} [\chi(X_t^\eta - x) g(X_s^\eta, s)] d\eta ds \end{aligned} \quad (2.7)$$

for $x \in \mathbb{R}^3$, where the Brownian fluid particles are defined in terms of the stochastic differential equation (1.1). In the approach of LES, one derives the evolution equation for the locally averaged velocity $\tilde{u}(x, t)$, namely the Navier-Stokes equations with the error term, and LES is then implemented by modelling the error. Taking advantage of the integral representation (2.7), which though is an implicit representation, we may devise a natural closure scheme without further modelling for the evolution of the locally averaged velocity $\tilde{u}(x, t)$.

More precisely, given a filter function χ , we run Brownian fluid particles with the locally averaged velocity $\hat{u}(x, t)$ defined by stochastic differential equation

$$d\hat{X}_t^\eta = \hat{u}(\hat{X}_t^\eta, t) dt + \sqrt{2\nu} dB_t, \quad \hat{X}_0^\eta = \eta, \quad (2.8)$$

$$\begin{aligned} \hat{u}(x, t) &= \int_{\mathbb{R}^3} \mathbb{E} [\chi(\hat{X}_t^\eta - x)] u_0(\eta) d\eta \\ &+ \int_0^t \int_{\mathbb{R}^3} \mathbb{E} [\chi(\hat{X}_t^\eta - x) \hat{g}(\hat{X}_s^\eta, s)] d\eta ds, \end{aligned} \quad (2.9)$$

where

$$\hat{g}(x, t) = -\nabla \hat{p}(x, t) + F(x, t), \quad (2.10)$$

and

$$\nabla \hat{p}(x, t) = \int_{\mathbb{R}^3} K_3(\hat{X}_t^\eta, x) \left(\sum_{i,j=1}^3 \frac{\partial \hat{u}^j}{\partial x_i} \frac{\partial \hat{u}^i}{\partial x_j} - \nabla \cdot F \right) \Big|_{(\hat{X}_t^\eta, t)} d\eta. \quad (2.11)$$

The equations (2.8, 2.9, 2.10, 2.11) compose a closed system which allows to calculate numerically approximate locally averaged velocity of an incompressible fluid flow.

If we utilise a Gaussian filter function χ , to update the approximate pressure $\hat{p}(x, t)$, terms $\frac{\partial \hat{u}}{\partial x}$ in $\nabla \hat{p}$ can be calculated simply by differentiating $\hat{u}(x, t)$ via (2.9).

3 Numerical schemes and numerical experiments

In this section we present several numerical experiments based on the scheme defined by (2.8, 2.9, 2.10, 2.11). For simplicity, we drop the hat script, and therefore define the following system

$$dX_t^\eta = u(X_t^\eta, t) dt + \sqrt{2\nu} dB_t, \quad X_0^\eta = \eta \quad (3.1)$$

where B is a Brownian motion on some probability space,

$$u(x, t) = \int_{\mathbb{R}^3} \mathbb{E} [\chi(X_t^\eta - x)] u_0(\eta) d\eta + \int_0^t \int_{\mathbb{R}^3} \mathbb{E} [\chi(X_t^\eta - x) g(X_s^\eta, s)] d\eta ds, \quad (3.2)$$

$$g(x, t) = -\nabla p(x, t) + F(x, t) \quad (3.3)$$

and the pressure gradient is updated by

$$\nabla p(x, t) = \int_{\mathbb{R}^3} K_3(X_t^\eta, x) \left(\sum_{i,j=1}^3 \frac{\partial u^j}{\partial x_i} \frac{\partial u^i}{\partial x_j} - \nabla \cdot F \right) \Big|_{(X_t^\eta, t)} d\eta. \quad (3.4)$$

In this scheme, the initial velocity u_0 and the external force F are given data. The whole scheme, which may be called the random LES, is determined by a filter function χ which must be chosen according to the mesh size when implement the simulation.

The initial velocity $u(x, 0)$ is given, so the initial pressure $p(x, 0)$ can be calculated directly, we choose external force F to be a constant so that $\nabla \cdot F = 0$.

Set mesh size $s > 0$, time step $\delta > 0$ and kinematic viscosity $\nu > 0$. For $i_1, i_2, i_3 \in \mathbb{Z}$, denote $x^{i_1, i_2, i_3} = (i_1, i_2, i_3)s$, $u^{i_1, i_2, i_3} = u(x^{i_1, i_2, i_3}, 0)$. In numerical scheme, we drop the expectation and use one-copy of Brownian particles. We discrete the stochastic differential equation (3.1) following Euler scheme: for $t_i = i\delta, i = 0, 1, 2, \dots$.

$$X_{t_k}^{i_1, i_2, i_3} = X_{t_{k-1}}^{i_1, i_2, i_3} + \delta u(X_{t_{k-1}}^{i_1, i_2, i_3}, t_{k-1}) + \sqrt{2\nu}(B_{t_k} - B_{t_{k-1}}), \quad X_0^{i_1, i_2, i_3} = x^{i_1, i_2, i_3}$$

where $X_{t_k}^{i_1, i_2, i_3}$ denotes $X_{t_k}^{x^{i_1, i_2, i_3}}$ for simplicity. Then integral representations in (3.2), and (3.4) can be discretised as follows:

$$u(x, t_k) = \sum_{i_1, i_2, i_3} s^3 \chi(X_{t_k}^{i_1, i_2, i_3} - x) u^{i_1, i_2, i_3} + \sum_{i_1, i_2, i_3} \sum_{j=1}^k s^3 \delta \chi(X_{t_k}^{i_1, i_2, i_3} - x) g(X_{t_{j-1}}^{i_1, i_2, i_3}, t_{j-1})$$

and

$$g(x, t_k) = - \sum_{i_1, i_2, i_3} s^3 K(X_{t_k}^{i_1, i_2, i_3}, x) \sum_{i,j=1}^3 A_i^j(X_{t_k}^{i_1, i_2, i_3}, t_k) A_i^j(X_{t_k}^{i_1, i_2, i_3}, t_k) + F,$$

where

$$A(x, t_k) = \sum_{i_1, i_2, i_3} s^3 \nabla_x \chi(X_{t_k}^{i_1, i_2, i_3} - x) u^{i_1, i_2, i_3} + \sum_{i_1, i_2, i_3} \sum_{j=1}^k s^3 \delta \nabla_x \chi(X_{t_k}^{i_1, i_2, i_3} - x) g(X_{t_{j-1}}^{i_1, i_2, i_3}, t_{j-1}).$$

We next carry out several numerical experiments by using the previous scheme.

3.1 Numerical experiments – laminar flows

By a laminar flow we mean a viscous flow with a small Reynolds number, where the Reynolds number is defined by $Re = \frac{U_0 L}{\nu}$, where U_0 is the main stream velocity and L is the length scale. In our experiment, $\nu = 0.15$, $Re = 800$, length scale $L = 2\pi$, so that $U_0 = \frac{\nu}{L} Re = 23.8$. The mesh size $s = \frac{2\pi}{20} \sim L \sqrt{\frac{1}{Re}}$. and the time step $\delta = 0.001$. The numerical experiment is demonstrated at times $t = 0.3, t = 0.6, t = 0.9$. We set the initial velocity to be of the form $u(x, 0) = (U_0 \sin(2x_1), U_0 \cos(2x_1), 0)$, and set force $F = (10, 10, -9.81)$. The velocity field and the vorticity field are shown in Figure 1 and Figure 2.

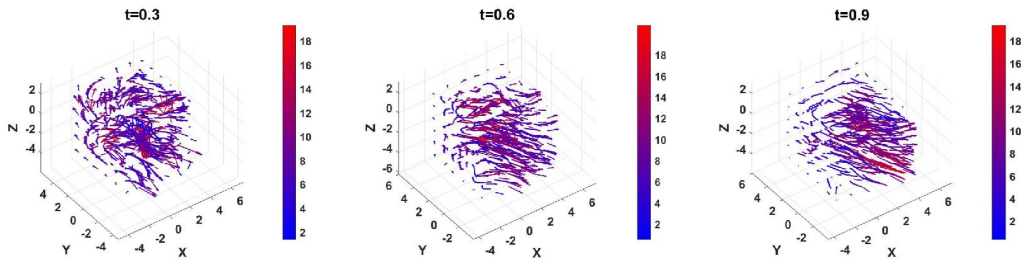


Figure 1: Velocity fields of incompressible viscous flows on \mathbb{R}^3

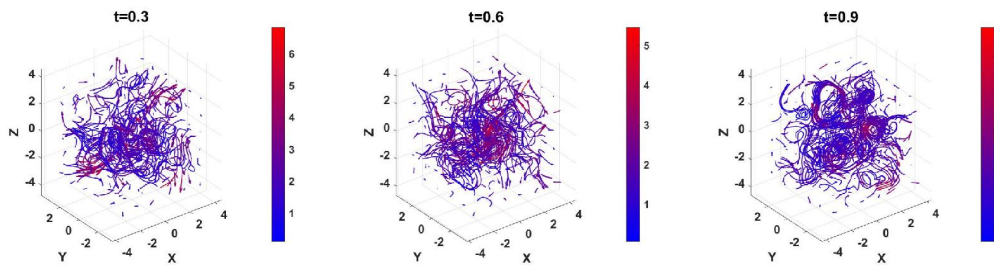


Figure 2: Vorticity fields of incompressible viscous flows flows on \mathbb{R}^3

Figure 1 and Figure 2 show a laminar flow where the velocity varies smoothly, while the vorticity field changes relatively fast, which is consistent with the real flow in question. To view the flows clearly, we also print sections of the vector fields with the plane $z = 0$, plane $x = 0$, and the plane $y = 0$ in Figure 3, Figure 4, Figure 5 respectively.

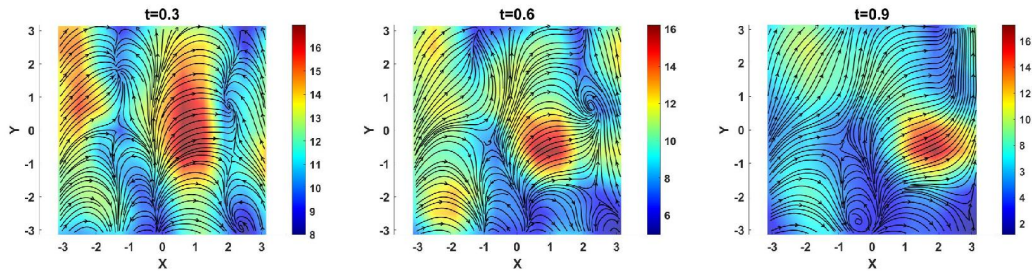


Figure 3: Section Velocity fields of incompressible viscous flows on plane $z = 0$

As shown in Figure 3, because of the initial conditions, there are more vortices and complex flows occurring on the plane $z = 0$. The external force F applying to this laminar flows system is not strong enough, so the fluid changes are not particularly large.

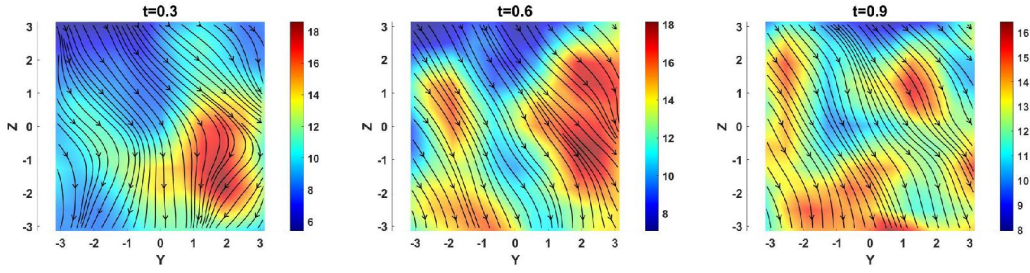


Figure 4: Section Velocity fields of incompressible viscous flows on plane $x = 0$

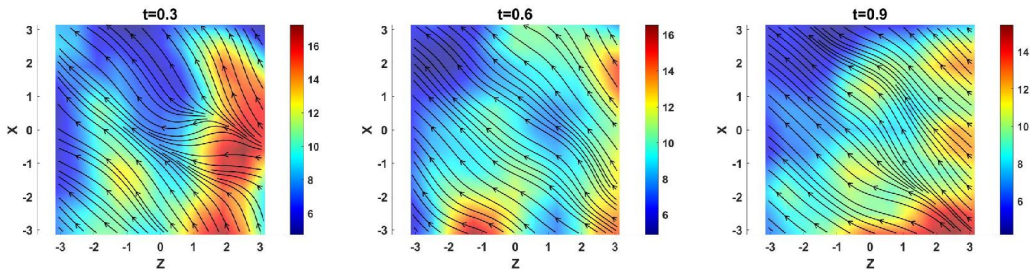


Figure 5: Section Velocity fields of incompressible viscous flows on plane $y = 0$

The initial vorticity is apparent only in plane $z = C$ (C is constant), it is clear that more obvious vortexes and changes appear in the horizontal section because the force F applying into the flows system is constant. So, in plane $x = C$ and plane $y = C$, the fluid shows a tendency to flow normally, flows in the direction of the external force.

3.2 Turbulence flows

We present a numerical experiment showing a 3D turbulent flow, a flow with large Reynolds number. In the numerical experiment, $\nu = 0.15$, $Re = 4500$, length scale $L = 2\pi$, so that $U_0 = 107.5$. The mesh size $s = \frac{2\pi}{40}$, and the time step $\delta = 0.001$. The numerical experiment results are demonstrated at times $t = 0.05, t = 0.1, t = 0.15$. We set the initial velocity to be of the form $u(x, 0) = (U_0 \sin(2x_1), U_0 \cos(2x_1), 0)$, set force $F = (50, 50, -9.81)$. The velocity field and vorticity field are shown in Figure 6 and Figure 7.

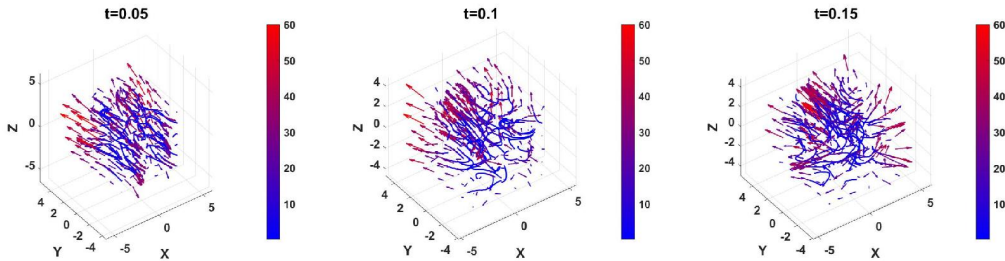


Figure 6: Velocity fields of incompressible viscous flows on \mathbb{R}^3

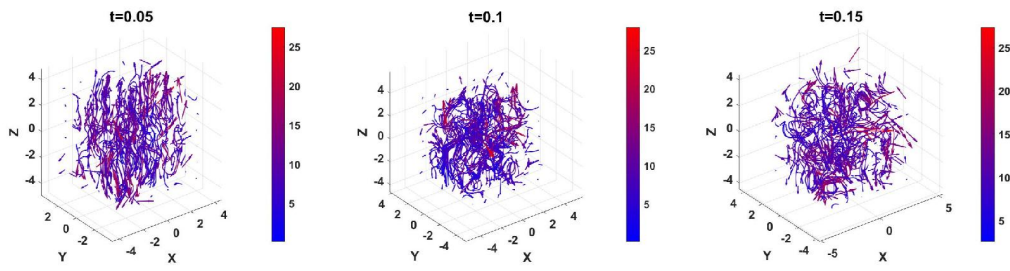


Figure 7: Vorticity fields of incompressible viscous flows on \mathbb{R}^3

In turbulence flows, given the initial velocity, the vorticity is larger and the vorticity field is more chaotic under larger velocity fields and external forces. To view the flows clearly, we also print the vector fields of section with plane $z = 0$, plane $x = 0$, and plane $y = 0$ in Figure 8, Figure 9, Figure 10 respectively.

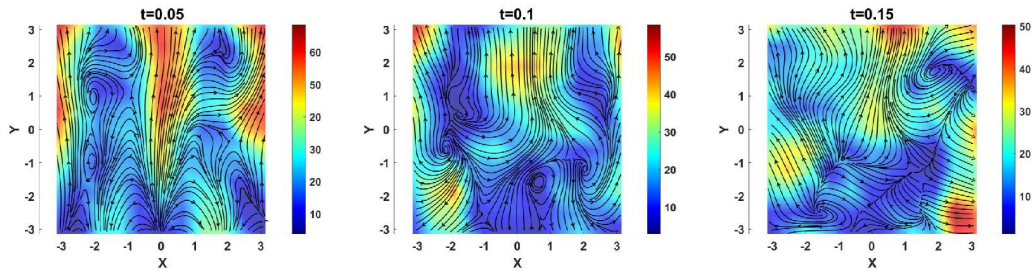


Figure 8: Section Velocity fields of incompressible viscous flows on plane $z = 0$

Compared with laminar flow, more eddies and more complex flows appear on plane $z = 0$ in turbulence flow. Because the initial velocity and force are relatively large, the changes in the fluid are also more significant.

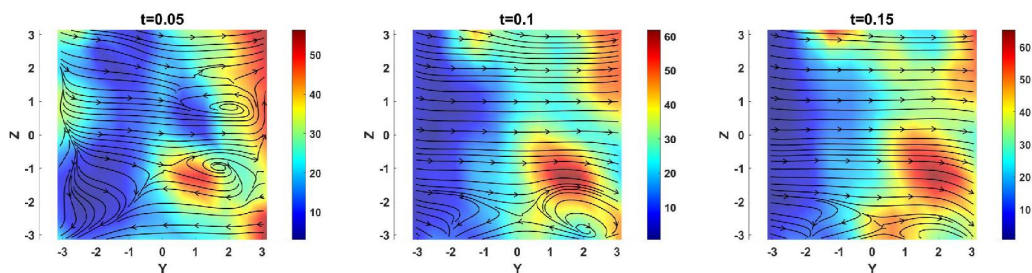


Figure 9: Section Velocity fields of incompressible viscous flows on plane $x = 0$

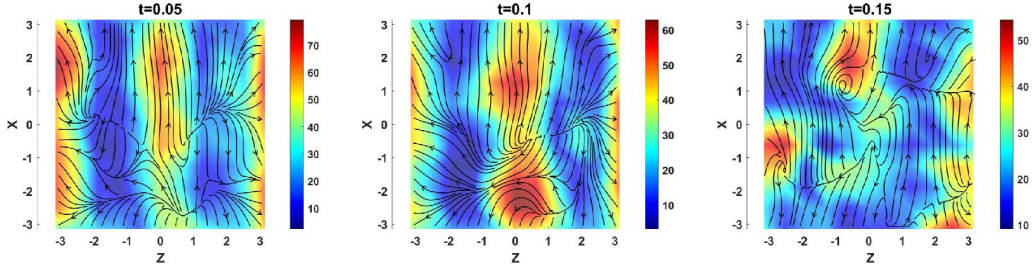


Figure 10: Section Velocity fields of incompressible viscous flows on plane $y = 0$

Although the initial vorticity is only given in plane $z = C$ (C is constant), there are still fewer vortices and changes appearing in plane $x = C$ and plane $y = C$ under turbulence case and large external force.

4 Appendix

In this section, we derive the integral representation theorem which is the key ingredient in the present work.

Suppose $b(x, t)$ is a time-dependent divergence-free vector field on $\mathbb{R}^d \times [0, \infty)$, i.e. $\nabla \cdot b = 0$. Let $L_b = \nu \Delta + b \cdot \nabla$, then the L^2 -adjoint operator of forward heating operator $L_b - \partial_t$ coincides with backward heat operator $L_{-b} + \partial_t$ (see [4] for details). Let $\Omega = C([0, \infty), \mathbb{R}^d)$ be the continuous path space in \mathbb{R}^d , define $X_t : \Omega \mapsto \mathbb{R}^d$ be the coordinate process on Ω . Let $\mathcal{F}_t^0 = \sigma\{X_s : s \leq t\}$ be the smallest σ -algebra on Ω and $\mathcal{F}^0 = \sigma\{X_s : s < \infty\}$. Then $\mathcal{F}^0 = \mathcal{B}(\Omega)$ is the Borel σ -algebra on Ω generated by the uniform convergence over any bounded subset $[0, \infty)$. We assume $b(x, t)$ is bounded and Borel measure, then for $\xi \in \mathbb{R}^d$, $\tau \geq 0$, there is a unique probability measure $\mathbb{P}_b^{\xi, \tau}$ on (Ω, \mathcal{F}^0) such that

$$\mathbb{P}[X_s = \xi \text{ for } s \leq \tau] = 1$$

and

$$M_t^{[f]} = f(X_t, t) - f(X_\tau, \tau) - \int_\tau^t (L_b f)(X_s, s) ds$$

is a local martingale ($\tau \leq t$) under probability measure $\mathbb{P}_b^{\xi, \tau}$, where $f \in C_b^{2,1}(\mathbb{R}^d \times [0, \infty))$. $\mathbb{P}_b^{\xi, \tau}$ is called L_b -diffusion, and L_b is called the infinitesimal generator of $\mathbb{P}_b^{\xi, \tau}$ [15]. $\mathbb{P}_b^{\xi, \tau}$ can be constructed as the weak solution of stochastic differential equation

$$dX_t = b(X_t, t)dt + \sqrt{2\nu}dB_t, \quad X_\tau = \xi,$$

where B is a Brownian motion on probability space. Let $p_b(\tau, \xi; t, x)$ denote the transition function of L_b -diffusion, which is positive and continuous in all arguments for $\tau < t$ and $\xi, x \in \mathbb{R}^d$, in the sense that

$$p_b(\tau, \xi; t, x)dx = P(\tau, \xi, t, dx) = \mathbb{P}_b^{\xi, \tau}[X_t \in dx],$$

see [15] for details. Given $T > 0$, $\mathbb{P}_b^{\xi, \tau}[\cdot | X_T = \eta]$ denotes the conditional law of the L_b -diffusion. Then it has been established in [11] that the conditional law $\mathbb{P}_b^{\xi, 0 \rightarrow \eta, T}$ coincide with the conditional law $\mathbb{P}_{-b^T}^{\eta, 0 \rightarrow \xi, T} \circ \tau_T$ up to a time reverse at T , where $b^T(x, t) = b(x, (T - t)^+)$. In fact it follows immediately from the fact that, since b is divergence-free,

$$p_{-b^T}(s, x; t, y) = p_b(T - t, y; T - s, x)$$

for $0 \leq s < t \leq T$ and $x, y \in \mathbb{R}^d$, cf. [11] for details.

Let $\Psi(x, t)$ be the smooth solution of parabolic equation

$$\left(L_{-b} - \frac{\partial}{\partial t}\right) \Psi + f = 0 \quad \text{in } \mathbb{R}^d \times [0, \infty) \quad (4.1)$$

where $f(x, t)$ is $C^{2,1}$ -function. Assume that $b(x, t)$ is $C^{2,1}$ and bounded, then we have the following theorem.

Theorem 4.1. *Suppose $b(x, t)$ is divergence-free, that is, $\nabla \cdot b = 0$ in the sense of distribution on \mathbb{R}^d . Then*

$$\begin{aligned} \Psi(\xi, T) &= \int_{\mathbb{R}^d} p_b(0, \eta; T, \xi) \Psi(\eta, 0) d\eta \\ &+ \int_0^T \int_{\mathbb{R}^d} \mathbb{P}_b^{\eta, 0} [f(X_t, t) | X_T = \xi] p_b(0, \eta; T, \xi) d\eta dt \end{aligned} \quad (4.2)$$

for $\xi \in \mathbb{R}^d$ and $T > 0$.

Proof. First, we construct a diffusion associated with time-reversal vector field b^T by solving the following SDE:

$$d\tilde{X}_t^\xi = -b(\tilde{X}_t^\xi, T-t) dt + \sqrt{2\nu} dB_t, \quad \tilde{X}_0^\xi = \xi$$

whose infinitesimal generator is L_{-b^T} . Let $Y_t = \Psi(\tilde{X}_t^\xi, T-t)$, then by Itô formula and equation 4.1

$$Y_t = Y_0 + \sqrt{2\nu} \int_0^t \nabla \Psi(\tilde{X}_s^\xi, T-s) \cdot dB_s - \int_0^t f(\tilde{X}_s^\xi, T-s) ds$$

Taking expectation of both sides and $t = T$, we have

$$\begin{aligned} \Psi(\xi, T) &= \mathbb{E} \left[\Psi(\tilde{X}_T^\xi, 0) \right] + \int_0^T \mathbb{E} \left[f(\tilde{X}_t^\xi, T-t) \right] ds \\ &= J_1 + J_2 \end{aligned}$$

By using conditional expectation, we may write

$$\begin{aligned} J_2(\xi, T) &= \int_0^T \int_{\mathbb{R}^d} \mathbb{E} \left[f(\tilde{X}_t^\xi, T-t) | \tilde{X}_T^\xi = \eta \right] \mathbb{P} \left[\tilde{X}_T^\xi \in d\eta \right] dt \\ &+ \int_0^T \int_{\mathbb{R}^d} \mathbb{E} \left[f(\tilde{X}_t^\xi, T-t) | \tilde{X}_T^\xi = \eta \right] p_{-b^T}(0, \xi; T, \eta) d\eta dt \end{aligned}$$

Similarly

$$J_1(\xi, T) = \int_{\mathbb{R}^d} \Psi^i(\eta, 0) p_{-b^T}(0, \xi; T, \eta) d\eta.$$

Since $\nabla \cdot b = 0$, we have $p_b(0, \eta; T, \xi) = p_{-b^T}(0, \xi; T, \eta)$, we can get

$$J_1(\xi, T) = \int_{\mathbb{R}^d} \Psi(\eta, 0) p_b(0, \eta; T, \xi) d\eta$$

and

$$J_2(\xi, T) = \int_0^T \int_{\mathbb{R}^d} \mathbb{E} \left[f(\tilde{X}_t^\xi, T-t) | \tilde{X}_T^\xi = \eta \right] p_b(0, \eta; T, \xi) d\eta dt.$$

Let $\mathbb{P}_{-b^T}^{\xi, 0}$ be the distribution of \tilde{X}^ξ , and $\mathbb{P}_{-b^T}^{\xi, 0 \rightarrow \eta, T}$ is the conditional distribution under condition $\tilde{X}_T^\xi = \eta$, then we can rewrite J_2 as

$$J_2(\xi, T) = \int_0^T \int_{\mathbb{R}^d} \mathbb{P}_{-b^T}^{\xi, 0 \rightarrow \eta, T} [f(\psi(t), T-t)] p_b(0, \eta; T, \xi) d\eta dt$$

which can be written as

$$J_2(\xi, T) = \int_0^T \int_{\mathbb{R}^d} \mathbb{P}_b^{\eta, 0 \rightarrow \xi, T} [f(\psi(T-t), T-t)] p_b(0, \eta; T, \xi) d\eta dt$$

Therefore after a change of variable for t to $T-t$,

$$J_2(\xi, T) = \int_0^T \int_{\mathbb{R}^d} \mathbb{P}_b^{\eta, 0 \rightarrow \xi, T} [f(\psi(t), t)] p_b(0, \eta; T, \xi) d\eta dt$$

which yields the integral representation 4.2. □

Data Availability Statement

No data are used in this article to support the findings of this study.

Declaration of Interests

The authors report no conflict of interest.

Acknowledgement

The authors would like to thank Oxford Suzhou Centre for Advanced Research for providing the excellent computing facility.

Bibliography

- [1] Chorin, A.J. 1973. Numerical study of slightly viscous flow. *Journal of Fluid Mechanics*, 57:785-796.
- [2] Cottet, G. -H., and Koumoutsakos, P. D. 2000 Vortex methods: theory and practice. *Cambridge University Press*
- [3] Deardorff, J. W. 1970. A numerical study of three-dimensional turbulent channel flow at large Reynolds numbers. *Journal of Fluid Mechanics*, 41(2), 453-480.
- [4] Friedman, A. 1964. Partial differential equations of parabolic type. Prentice-Hall, Inc.
- [5] Landau, L. D. and Lifshitz, E. M. 1987 Fluid mechanics. Second edition. Pergamon Press.
- [6] Li, J., Qian, Z. and Xu, M. 2023. Twin Brownian particle method for the study of Oberbeck-Boussinesq fluid flows. <https://arxiv.org/abs/2303.17260>.
- [7] Lesieur, M., Métais, O. and Comte, P. 2005, Large-eddy simulations of turbulence. Springer.
- [8] Majda, A. J. and Bertozzi, A. L. 2002 Vorticity and incompressible flow. *Cambridge University Press*.
- [9] Piomelli, Ugo; Elias Balaras. 2002. Wall-layer models for large-eddy simulations. *Annual Review of Fluid Mechanics*, 34 (34): 349–374.
- [10] Pitsch, Heinz. 2006. Large-Eddy Simulation of Turbulent Combustion. *Annual Review of Fluid Mechanics*, 38 (1): 453–482.

- [11] Qian Z., Süli E., and Zhang Y. 2022. Random vortex dynamics via functional stochastic differential equations. *Proc. R. Soc. , A478*: 20220030.
- [12] Qian, Z. 2022. Stochastic formulation of incompressible fluid flows in wall-bounded regions. arXiv:2206.05198
- [13] Reynolds, O. 1895. On the dynamical theory of incompressible viscous fluids and the determination of the criterion. *Philosophical Transactions of the Royal Society of London*, 186: 123–164.
- [14] Smagorinsky, Joseph. 1963. General Circulation Experiments with the Primitive Equations. *Monthly Weather Review*, 91 (3): 99–164.
- [15] Stroock, D. W. and Varadhan, S.R.S. 1979 *Multidimensional diffusion processes*. Springer.
- [16] Volker John. 2004. *Large Eddy Simulation of Turbulent Incompressible Flows*. Springer.